Electric Power Systems Research 111 (2014) 96–102

Contents lists available at ScienceDirect

Electric Power Systems Research

journal homepage: www.elsevier.com/locate/epsr

Automatic capacitor bank identification in power distribution systems

Alexandre Perera-Lluna[a,*], Karthick Manivannan[b], Peng Xu[b], Ricardo Gutierrez-Osuna[c], Carl Benner[b], B. Don Russell[b]

[a] Automatic Control Department (ESAII), Universitat Politècnica de Catalunya, 08028 Barcelona, Spain
[b] Department of Electrical and Computer Engineering, Texas A&M University, College Station, TX 77843, USA
[c] Department of Computer Science, Texas A&M University, College Station, TX 77843, USA

ARTICLE INFO

Article history:
Received 9 July 2010
Received in revised form
16 December 2013
Accepted 2 February 2014
Available online 12 March 2014

Keywords:
Capacitor switching
Power distribution
Clustering
ISODATA

ABSTRACT

Tracking the performance and health of capacitor banks in distribution systems is a challenging task due to their high number and the widespread geographical distribution of feeder circuits. In this work we propose a signal processing technique capable of identifying and characterizing the number of capacitor banks connected to a standard North-American feeder circuit. The way the technique is applied allows a real-time remote monitoring of their operation, automatically identifying the switching activity for each capacitor bank connected. The technique is based on an unsupervised clustering of the three phase reactance step magnitudes. We demonstrate that using only passive monitoring of conventional substation bus PTs and feeder CTs, without any communication, nor visual inspection, to individual banks, it is possible to predict the number of capacitor banks on the distribution feeder and track their performance and activity over time.

1. Introduction

Capacitor banks are common devices in power distribution systems. They provide reactive power, thereby improving power factor, reduced line loses, improved feeder voltage profile, and lower power line loadings. In order to obtain optimal power factor correction and voltage profile, banks of various sizes are selectively placed along each feeder. Once in operation, unmonitored capacitor banks are difficult to evaluate and their real performance is often unknown. While sophisticated systems provide communication to each and every bank for remote monitoring and control, this practice is expensive and not widespread in the electric utility industry.

Farag et al. performed an extensive statistical study of capacitor banks and other components. The authors investigated failure modes, reliability levels and failure causes for a population of more than 2900 capacitor banks during a period of 10 years (1980–1990) [1]. The authors published statistics of the location of the failures, capacitor banks being the component more prone to present a failure (70.0%), followed by oil switches (12.3%), clocks (3.5%), controllers (3.5%) and jumpers (1.7%). The sources of these failures were identified to be main insulation breakdown (92.4%), oil leaking, which also leads to a main insulation breakdown (5.2%) and broken bushings (2.4%). The study also provided statistics related to the device quality, in form of the average failure rates (*Fr*), which ranged from *Fr* = 0.715% to 2.150% depending on the manufacturer. Given the high number of banks that can be found in power distribution networks and the economical impact of a bank failure, which most of times remains unnoticed, these statistics provide a justification for further research on novel cost-effective methods for locating and monitoring sets capacitor banks in a distribution line.

A number of publications addressing different aspects related to capacitor banks are found in literature. These range from the optimization of capacitor allocation in the distribution lines [7,9], switching control techniques [11], the impact of the switched capacitors on customer systems [4,8]. Comparatively, there are a limited number of publications on warning systems for capacitor banks aimed at the identification, monitoring and detection faults related to capacitor banks in power distribution systems, and most of the existing methods rely on a sensing device placed near -or inside- the capacitor bank. Lee et al. [5] used a modified impedance relay to provide early warning based on a safety operation zone for capacitor bank protection. Sochuliakova et al. [12] developed methods for locating the placing of capacitor banks in radial systems from the analysis of the transient frequencies. The method allowed the use of a single monitoring device at substation level although the results of the analysis required the measurement of the line inductance from the customer to the capacitor, which may

* Corresponding author. Tel.: +34 4016963; fax: +34 4017045.
E-mail addresses: alexandre.perera@upc.edu, aperera@gmail.com (A. Perera-Lluna), karthick@ece.tamu.edu (K. Manivannan), ppengxu@gmail.com (P. Xu), rgutier@cs.tamu.edu (R. Gutierrez-Osuna), carl.benner@tamu.edu (C. Benner), bdrussell@tamu.edu (B.D. Russell).

0378-7796/$ – see front matter © 2014 Elsevier B.V. All rights reserved.
http://dx.doi.org/10.1016/j.epsr.2014.02.003

depend on the distribution line and geometry. Santoso et al. contributed with a different method for bank identification based on the installation of multiple power quality monitors among the line connected to a feeder [13]. Authors demonstrated that, given a capacitor switch event, each power quality monitor could determine whether the bank was placed upstream or downstream from the distribution line. Given that all monitors were placed strategically along the distribution line, it was possible to approximate which bank was activated/deactivated by using the simultaneous information provided by the monitors.

The technique proposed in this paper enables the remote identification and monitoring of capacitor banks using measurements performed only in the substation, with no communication to the banks deployed in the branch and with no prior knowledge of the number and size of the banks deployed. We propose the use of a single monitor device per feeder, as opposed to individual monitoring devices per capacitor banks, combined with pattern recognition techniques for monitoring, detecting and locating grounded capacitor bank failures. To that task we employ a clustering-based technique capable of: (1) grouping capacitor switch events based on the similarity of their transient signals, (2) determining the number of clusters observed at a particular feeder circuit, and (3) characterizing the capacitor size at each phase. The technique can thereby be employed to enumerate and characterize all capacitor banks in a feeder circuit without prior knowledge of their existence devices. The automatic identification and monitoring allows for future localization of abnormalities and failure prevention in capacitor banks at distribution lines.

2. Materials and methods

This work is part of a large-scale project sponsored by EPRI (Electric Power Research Institute, Palo Alto, CA, USA), which is aimed at providing tools for distributed fault anticipation (DFA) in power distribution lines. Within the framework of this project, a number of custom-designed signal acquisition modules have been installed in different feeders from multiple utilities. Each of these modules captures a variety of electrical signals that can be divided into two main groups:

- *Triggered by an event.* Each time that a disturbance is seen by the module, a signal is triggered and a number of waveforms are stored in a capture file. These waveforms include current, voltage, RMS current and voltage, real (P), apparent (S) and reactive (Q) power, and high frequency band energy ($f_s > 2$ kHz) data in the time window of the trigger. Typical capture lengths are 6 s including one second prior to trigger.
- *Statistics.* The system also captures multiple statistics (maximum, minimum, averages and standard deviations) of several variables every 15 min. These variables include power related signals (RMS voltage, RMS current, P, S, Q) plus frequency related information for the current signals, as well as weather conditions (temperature, humidity, rainfall, wind speed and wind direction).

All variables for both groups, *Triggered by an event* and *statistical*, are acquired for the three phases plus neutral where applicable. Data acquisition modules are installed on each feeder in selected substations, and are controlled from a master station at Texas A&M University (TAMU) by means of a TCP/IP connection over digital subscriber lines (DSL). The collection of all captured files is stored locally, and periodically transmitted to TAMU for further processing and archival purposes. Fig. 1 shows an example of a captured waveform. In this case, the acquisition was triggered by a grounded capacitor switch-off event, as evidenced by the clear step in reactive power (dQ_x) in all three phases. Following capture and event signal

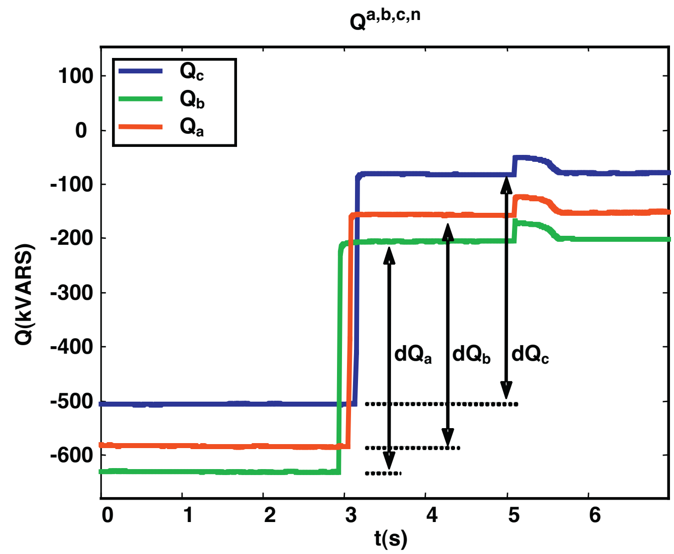

Fig. 1. Reactive power (Q) waveform for a capacitor switch off.

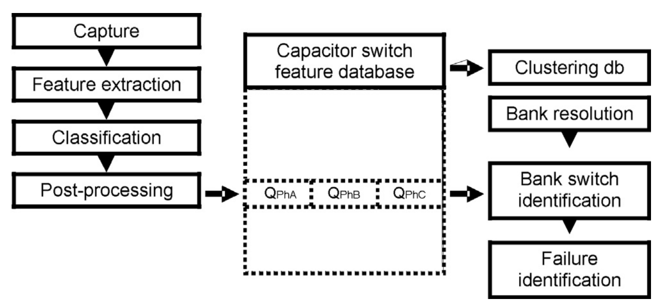

Fig. 2. General overview of the data processing path.

data, undergoes a series of processing steps, summarized in Fig. 2. From this feature set, a classifier algorithm will label each capture as belonging to "capacitor switch" category or "others". Captures labeled as capacitor switches are passed to a post-processing stage that computes a series of features that feeds a database, which is *database-mined* with the tools proposed in this work. The number and characteristics of the banks in a given circuit are then extracted by means of a clustering algorithm and a bank resolution post-processing step, as described in Section 2.2. Once this information is available, it is then possible to monitor the evolution of the banks in a feeder line. The different stages of the processing architecture are described with more detail in the following sections.

2.1. Recognition of capacitor bank events

Four features are extracted from the power (P), reactive power (Q), current *RMS* (I_{RMS}) and voltage *RMS* (V_{RMS}) waveforms:

- The step change between the beginning and the end of the waveform, S^{dif}
- The maximum and minimum value relative to the start of the waveform, S^{max}, S^{min}
- The maximum value of the signal relative to the minimum value, S^{mdif}

This feature extraction is done for each phase. In order to prevent the feature extraction step and further processing to be phase dependant, only the maximum value for the three phases is

Table 1
Confusion matrix for the capture database. 1-NN (loo).

Predicted\Real	Cap-Sw on	Cap-Sw off	Others
Cap-Sw on	382	0	16
Cap-Sw off	0	189	4
Others	8	7	3632
	98%	96%	99%

considered as a feature, e.g. $S^{\max} = \max(S_a^{\max}, S_b^{\max}, S_c^{\max})$. The values of the neutral, when applicable are included separately. Experts at TAMU manually classified a set of 4238 captures. This capture set was acquired between March 1 and December 2, 2003 by the DFA system from 26 feeders on eight different utilities in the US, placed on different geographical locations. From these captures, 196 events were classified as capacitor switch-off and 390 were classified as capacitor switch-on. This database was used to train a pattern classifier to discriminate between capacitor switching events and all remaining events in the database. The event classification is performed in two steps. First, a subset of relevant features is constructed using machine-learning techniques [6]. Second, a nearest neighbor classifier is applied to the reduced set and used to classify future events. The automatic selection of the feature subset was computed through a model selection algorithm, employing a sequential floating technique known as SFFS (for sequential forward floating selection, see [10]). The SFFS algorithm starts with an empty feature set. In the first iteration, it finds the single feature that provides the best classification performance on the data. After this feature has been selected, the next feature is selected following the same criteria in what is called a forward step. Iteratively, if the classification performance is improved by removing some of the features in the new dataset, the algorithm performs a backward step by removing that particular feature. SFFS keeps dynamically increasing and decreasing the number of features through forward and backward steps until no improvement is found, or the algorithm has reached the maximum number of desired of elements (see [6] for further details). By using the abovementioned procedure, an optimum number of 10 features were automatically selected: Q^{diff}, P^{diff}, $P^{\max}$, Q^{mdif}, P^{mdif}, V^{dif}_{RMS}, V^{mdif}_{RMS}, $I^{mdif}_{N,RMS}$, I^{mdif}_{RMS}, $V^{\max}_{RMS}$.

Looking at the sequence in which the features are sequentially added to the subset, it is clear that information is contained both in the reactive and the real power. These results are consistent with the behavior of the signals under a capacitor switch event, consisting of an abrupt change in reactive power while keeping the change in apparent power restively small ($\left|dQ\right| / \left|dP\right| \uparrow$). This information will reside mainly in the plane given by Q^{dif} and P^{dif}. We believe that the rest of features are included to lower the false positive rate for the capture set classified as "others". The final performance of the classifier stage is summarized in form of a confusion matrix, given in Table 1.

2.2. *Identification of capacitor banks connected to the distribution lines*

Once an event has been classified as a capacitor switch by the nearest neighbor classifier described in the previous section, we consider only the features concerning differential reactive power Q^{dif} per each on of the phases are preserved to perform capacitor bank identification. These features will be referred as $dQ_{a,b,c}$ from this section onwards. The rest of features can be discarded since they mainly aid in the discrimination between capacitor switch events and rest of events.

In a first attempt, the number of capacitor banks in a feeder circuit may be estimated from the probability distribution (e.g., a histogram) of the reactive power steps (dQ) for each phase. Assuming that the banks are of different size, and that each of them has triggered a sufficient number of times, each bank can be detected by a peak in the histogram. This is illustrated in Fig. 3, including data from a feeder collected between July 1, 2003 and March 3, 2004. During this period, a total of 1029 capacitor switch events were captured by the system. Histograms of the reactive power steps for each phase are shown in Fig. 3, where significant discrepancies between the three phases can be noticed. The histogram for phase A shows four clear peaks at 0.42 MVAR, 0.39 MVAR, 0.32 MVAR and 0.14 MVAR. However, phases B and C show no indication of activity in the 0.39 MVAR and 0.42 MVAR range, but a weak peak can be detected at 0.30 MVAR in phase B. This example illustrates the shortcomings of attempting to identify capacitors on the basis of their activity per phase.

Manufacturers allow certain tolerances in the sizes of the capacitors for each phase. These may be as large as a 15% between the maximum and the minimum of the values of the capacitors per each phase. As a result, similar banks are likely to be confounded in the same peak.

To address this issue, we propose to use the information from these tolerances through the introduction of a novel multivariate identification method. This method is based on a key observation: the specific tolerances on each phase of a capacitor bank can be treated as an identifying signature for the bank.

This approach is best illustrated by plotting an instance of differential change in reactance against another (dQ_i vs. dQ_j). Switching events from an ideal capacitor bank will produce equal dQ in all three phases and, therefore, will lead to a scatter plot with activity aligned with the main diagonal ($dQ_i = dQ_j$) for different capacitors. Real capacitor switches, however, will display activity outside this diagonal due to the manufacturing tolerances. As an example, the scatter plot of dQ_c vs. dQ_b for a bank in Fig. 3 shows two clear groups of activity at $dQ_c = dQ_b = 0.3$ MVAR and $dQ_a = dQ_b = 0.15$ MVAR (see Fig. 4(a)). In contrast, the scatter plot of dQ_a vs. dQ_b (Fig. 4(b)) shows three groups of switching activity: a first group with a step of $dQ_a = 0.4$ MVAR and $dQ_b = 0.3$ MVAR, a second group with balanced activity at $dQ_a = dQ_b = 0.33$ MVAR, and a third cluster caused by a smaller bank that switches with $dQ_a = dQ_b = 0.15$ MVAR. These scatter plot alone does not provide sufficient information to determine whether the circuit contains three separate capacitor banks, or a single capacitor bank whose reactance step is changing due to a malfunction. Fortunately, the data acquisition system provides a time stamp for each event, which can be used to disambiguate between these two situations. The clusters observed in Fig. 4 can be automatically extracted using statistical pattern recognition techniques.

Formally, each switching event can be described by a feature vector $dQ = (dQ_a, dQ_b, dQ_c)$ in three-dimensional space. Groups of joint activity can be extracted through multivariate clustering. If the number of clusters (i.e. capacitor banks) was known, a partition of all the events can be obtained through of a *k-means* algorithm. However, the determination of the precise number of capacitor banks is an unknown variable.

We have employed an extension of the *k-means* algorithm known as ISODATA, which relaxes the a priori constraint that the number of clusters be known and fixed [2]. ISODATA automatically determines the number of clusters through a series of merge and split heuristics [3]. The algorithm works with four parameters: k, the first estimate of the number of centers; n_0, the minimum number of patterns per cluster; s_0, the splitting control parameter and d_0, the merging parameter. s_0 controls when a cluster should be split on the basis of its distribution: if the principal covariance component of a cluster is large enough compared to s_0, the cluster becomes eligible for splitting. On the other extreme, d_0 controls when two clusters are close enough to be eligible for being lumped: if the distance between two clusters is lower that d_0 these two

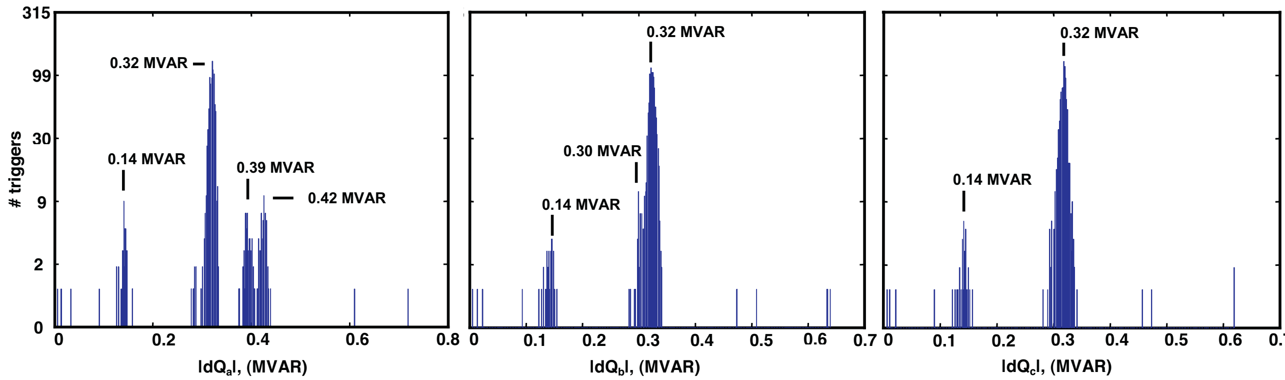

Fig. 3. Histogram of capacitor switches for each phase as a function of the absolute value of the relative reactive power $\left|dQ\right|$.

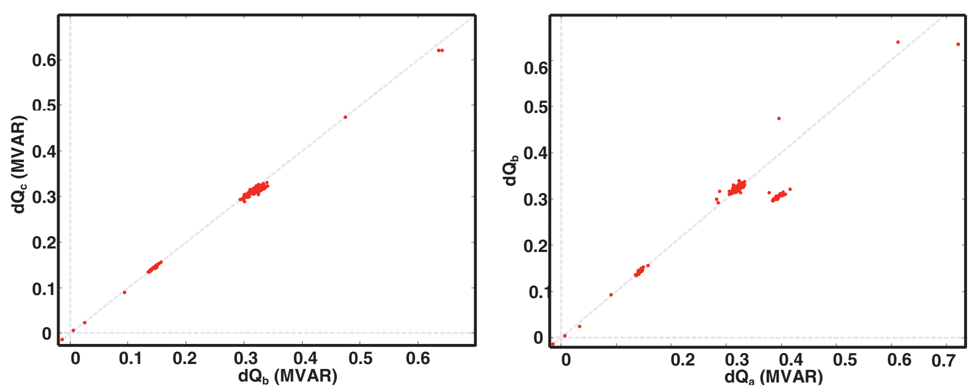

Fig. 4. Reactant power change for switch-off events ($dQ > 0$); (a) phase A vs. phase B, (b) phase B vs. phase C.

clusters are marked as candidates to a merge. Once the merge is done, the new cluster mean is the mean of the two centers. The main steps of the ISODATA algorithm are summarized in the following steps:

1. Initialization.
   a. Randomly assign each pattern to one of the initial k clusters
   b. UpdateMeans: compute mean vector for each cluster
2. Recluster. Assign each pattern to the closest cluster
3. Prune. Remove any cluster with less than n_0 patterns
4. UpdateMeans. Re-compute mean vectors from current assignment
5. Split. Test splitting conditions and split if conditions are met
6. If no split has been executed, test merging conditions and lump if conditions are met
7. Go to step 2 if the number of iterations have not been exceeded or convergence has not been reached;

The reader is referred to [2] for additional details. Please consider that ISODATA will find iteratively the optimal number of clusters, which means that it will estimate the existing number of banks connected to that particular line.

Appropriate values for the parameters (s_0, d_0) can be obtained from domain knowledge of what are considered as nominally identical banks. In our implementation, these parameters are set to $s_0 = (93\ \text{kVAR})^2$ and $d_0 = 10$ kVAR. An appropriate value for the initial number of banks was empirically determined to be $k = 8$. Those clusters with less than three samples were not considered by setting $n_0 = 3$. The clustering is performed with the features described earlier including all switching events in the database, which contains all capacitor events (energizing or switch-on and de-energizing or switch-off). A capacitor switch-*on* produces a reduction of the relative reactive power ($dQ < 0$), whereas, a capacitor switch-*off* produces a positive relative reactive power ($dQ > 0$). It is therefore

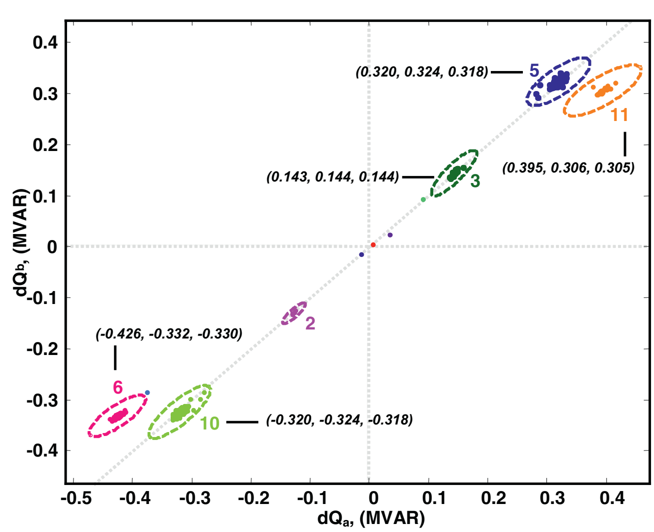

Fig. 5. Automatic cluster identification results for capacitor switch ON ($dQ < 0$) and OFF ($dQ > 0$) for feeder A.

to be expected that switch-on and switch-off events for the same bank will produce samples with similar $|dQ|$ but with different signs. This will create a cluster in the $dQ < 0$ region with all activity corresponding to a capacitor switch-on of a given bank, and another cluster in the region $dQ > 0$.

After the clustering algorithm is applied, specific information is extracted from each cluster: the mean vector of each cluster represents an estimate of the size of the capacitors at each phase, whereas the variance of the cluster provides a measure of the uncertainty of this estimate. The values for each phase are extracted from the assumption that all similar captures correspond to the same bank. Once the cluster information is extracted, the centroids are employed to identify the different banks. Also the properties of the samples associated to each centroid can be used to estimate to uncertainties of this measurement, as described in the results section.

It is necessary to employ a final bank resolution stage to match each cluster in $dQ_i > 0$ to clusters into $dQ_i < 0$ and decide whether these mirror clusters have been originated by the same or different bank.

Given a given cluster i defined by center of mass $\mathbf{dQ}_i = (dQ_{ai}, dQ_{bi}, dQ_{ci})$, the algorithm looks for the closest mirror cluster j that lies within a distance given by the sum of the uncertainty of the cluster i and the uncertainty of cluster j. The error in the estimation, or uncertainty, is computed by looking at the maximum direction of variance, which corresponds to the first eigenvalue of

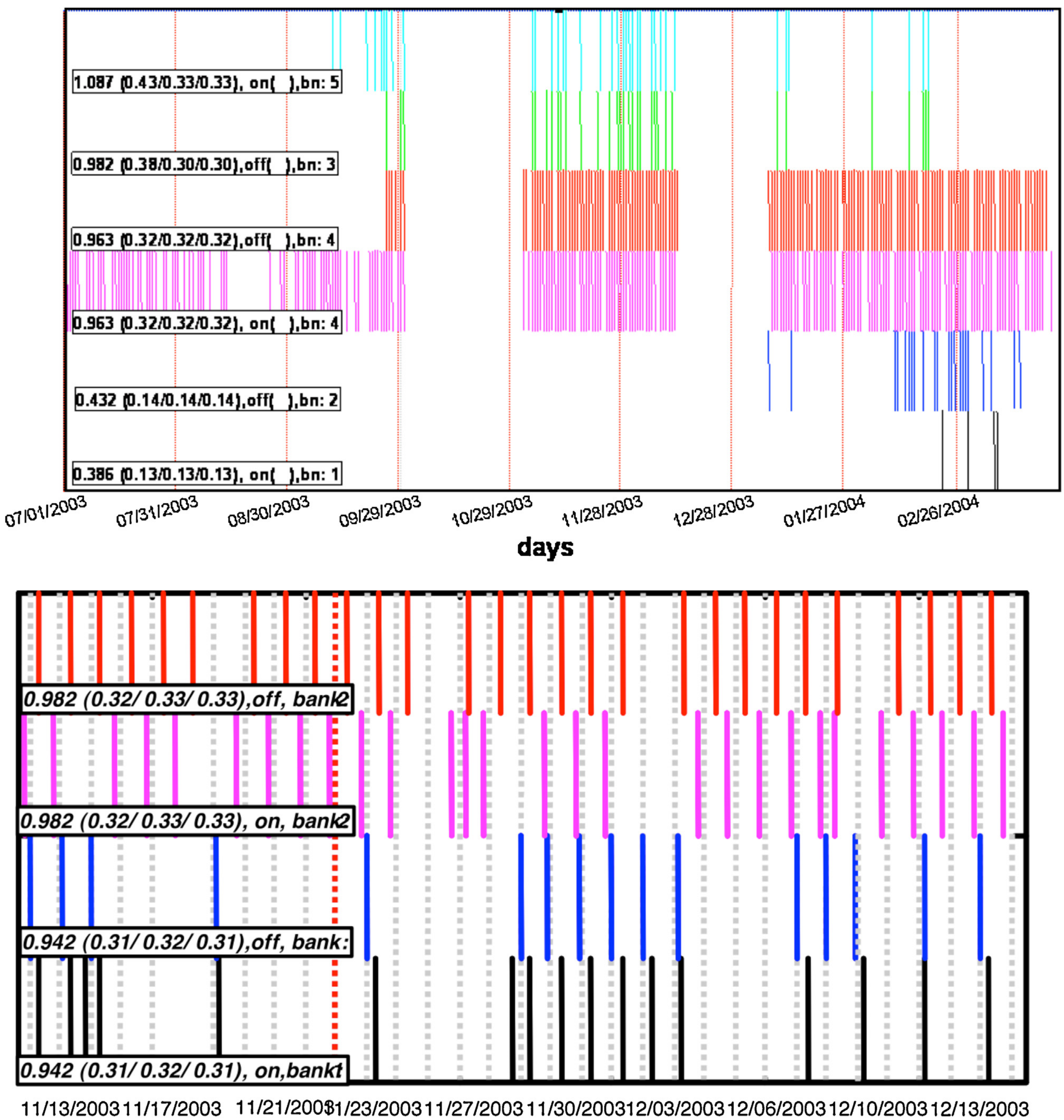

Fig. 6. Temporal switching activity for banks resolved in circuit A (top) and B (bottom). ([TS (SA, SB, SC), on/off, bn], where TS: bank size, SA/SB/SB: sizes for phases A, B, C, bn: bank number).

Table 2
Final capacitor bank groupings identified from cluster information from feeders A and B.

Feeder/Bank	Clusters	Size (MVAR)	PhA (kVAR)	PhB (kVAR)	PhB (kVAR)	Error (kVAR)	Samples
A/1	2	0.386	129	129	128	5.9	4
A/2	3	0.432	143	144	144	8.2	28
A/3	11	0.982	385	295	301	29.8	49
A/4	5, 10	0.963	320	324	318	12.0	885
A/5	6	1.087	426	332	330	8.0	56
B/1	7, 8	0.942	310	318	315	8.4	190
B/2	9, 10	0.982	322	331	328	5.2	310

the covariance matrix of the samples forming the cluster considered. If a mirror cluster $\boldsymbol{dQ_j}$ is found within the search distance, the bank size is finally computed as the mean between the two clusters $B_k = (\left|dQ_i\right| + dQ_j)/2$. If a mirror cluster is not found, the bank size is computed with the information about the cluster $B_k = \left|dQ_i\right|$. This rule is applied until all clusters have been processed and enumerated.

3. Results

We have applied the process described to the dataset from the same feeder as described in Section 2.2 (feeder A). ISODATA correctly identifies the main clusters that are shown in Fig. 5. Clusters 5 and 10 in the figure denote switch-on and switch-off events from the same bank, respectively. However clusters 6 and 11 are no assigned by the algorithm to the same bank since there is a difference of nearly 50 kVAR in the phase A switching steps: the size of the bank representing cluster 6 is dQ = (426 kVAR, 332 kVAR, 330 kVAR) whereas cluster 11 is dQ = (385 kVAR, 295 kVAR, 301 kVAR). A complete list of all detected banks, as well as bank size estimates, error estimates, and number of switching events is shown in Table 2 (A/1–5 entries).

The bank information extracted with help of the clustering algorithm permits to monitor the activity of the identified banks. This is achieved by looking at the closest cluster once a capture is processed, classified as a capacitor switch after the computation of their dQ signature. The temporal switching activity of feeder A for a period of 9 months is shown in Fig. 6. Noticeably, bank 4 evolves with a regular switching activity whereas banks 1, 2, 3 and 5 develop an irregular pattern of activity. It is known, based on information provided by the utility, which in the distribution line connected to feeder *A* we should find four banks with a size of 900 kVAR. The fact that some banks started switching at 430 kVAR and 386 kVAR is a clear sign of a bank malfunction. In the case of strict equally size banks, multiple capacitor-switch captures will converge into the same cluster. Although the method proposed here would not discriminate these cases, it may be possible to hypothesize that regularly switched capacitors, like banks controlled by timer based devices, will statistically distribute in the time margins programmed in the controller. Under this assumption, the switching time could be considered as an additional feature for a second-stage clustering. This method could help to provide additional discrimination for each cluster found by ISODATA.

The algorithm was also tested on data from a second feeder (feeder B) of the same substation as the described in Section 2.2. The database consisted of 509 capacitor-switching events. The utility indicated that in this case two 900 kVAR capacitor banks existed in this distribution line. The bank resolution algorithm correctly discovered two capacitor banks at 942 kVAR and 982 kVAR despite the close similarity between them (only a 4% difference). Final results for the two banks found by the algorithm are summarized in Table 2 (B/1 and B/2 entries). The algorithm correctly matched capacitor switch-on and switch-off clusters for each capacitor bank unit. The estimation error is smaller than 10 kVAR for both banks. A close-up temporal view of the bank activity for a period of 30 days is shown in Fig. 6 (bottom), where bank number 2 is found to switch regularly on a daily basis except for one out of every seven days in which no activation was sensed. On the other hand, Bank number 1 does not present such a regular activity. Moreover, the actual number of activations for that bank is lower, 190 switches for bank 1 vs. 310 for bank 2. This information could be useful to statistically check the performance and correct behavior of capacitor banks in the distribution line. The overall performance of the algorithm is good considering that the discrimination is done by means of a single acquisition system installed in the feeder and three features from every switch event.

4. Conclusion

Capacitor banks are broadly used in electrical power distribution systems. Their large number and the diversity of their locations in the US geography difficult the monitoring their performance and correct functioning. Moreover, certain bank malfunctions are silent for large periods of time as they are not visually noticeable and its finding requires expensive maintenance programs. Examples of these malfunctions are stuck capacitors producing single, two phase, or even no-phase switching, errors in the controllers producing abnormal high frequency switching, or damage in the capacitor that induces deviations in the capacitor bank size.

This paper has proposed a novel method aimed at identifying, characterizing and tracking of grounded capacitor banks connected to a power distribution line in a cost effective manner. The method only requires of a single acquisition device placed at the substation, and that the line fulfills the main hypothesis stated (banks are connected to the line like in the US power distribution grid, and these banks have tolerances large enough that they can be considered as an individualized pattern). The algorithm is based in a two-stage process. First, a classification algorithm recognizes a capacitor switch event from all others. At a second stage, the method looks for similarities within the set of capacitor switch events by means of a mathematical dynamic clustering of the three-phase reactive power steps generated by the bank activation/deactivation. The algorithm correctly resolves different bank in the circuit, with help of pattern recognition mathematics applied to the switching signature obtained from each bank.

From the information automatically extracted by the system, the proposed approach allows the computation of temporal activity profiles in an individualized manner. These maps permit further tracking of anomalies in the capacitor bank activity in an automated fashion or providing visual displays suitable for the analysis by human experts. The algorithm does not require supervision (for the clustering stage) and only requires a monitor module at the substation level, which permits the possibility of a mass scale application for monitoring purposes.

Acknowledgments

The authors gratefully acknowledge the support of the Electric Power Research Institute and EPRI's Member Utility Companies. Their support provides the data upon which this investigation is based. Participating utilities also provided support by investigating and helping to document failures, faults, and other recorded anomalies.

References

[1] A.S. Farag, C. Wang, T.C. Cheng, G. Zheng, Y. Du, L. Hu, B. Palk, M. Moon, Failure analysis of composite dielectric of power capacitors in distribution systems, IEEE Trans. Dielectr. Electr. Insul. 5 (4) (1998) 583–588.
[2] G. Ball, D. Hall, ISODATA: a novel method of data analysis and pattern classification, Technical Report, Stanford Research Institute, Menlo Park, CA, 1965.
[3] K. Fukunaga, Introduction to Statistical Pattern Recognition, 2nd ed., Academic Press, 1990.
[4] A.A. Girgis, C.M. Fallon, J.C. Rubino, R. Catoe, Harmonics and transient overvoltages due to capacitor switching, IEEE Trans. Ind. Appl. 29 (6) (1993) 1184–1188.
[5] W. Lee, T. Krishnan Narayanan, P. Maffetone, Didsayabutra, The design of a capacitor bank early warning system, IEEE Trans. Ind. Appl. 39 (2) (2003) 306–312.
[6] A. Jain, D. Zongker, Feature selection: evaluation, application, and small sample performance, IEEE Trans. Pattern Anal. Mach. Intell. 19 (2) (1997) 153–158.
[7] S.F. Mekhamer, M.E. El-Hawary, M.M. Mansour, M.A. Moustafa, S.A. Soliman, State of the art in optimal capacitor allocation for reactive power compensation in distribution feeders, in: Large Engineering Systems Conference on Power Engineering 2002 (LESCOPE 02), 1992, pp. 61–75.
[8] M.F. McGranaghan, T.E. Grebe, G. Hensley, T. Singh, M. Samotyj, Impact of utility switched capacitors on customer systems, Part II. Adjustable-speed drive concerns, IEEE Trans. Power Del. 6 (4) (1998) 1623–1628.
[9] K.N. Miu, H.D. Chiang, G. Darling, Capacitor placement, replacement and control in large-scale distribution systems by a GA-based two-stage algorithm, IEEE Trans. Power Syst. 12 (3) (1997) 1160–1166.
[10] P. Pudil, J. Novovicova, J. Kittler, Floating search methods in feature selection, Pattern Recogn. Lett. 15 (1994) 1119–1125.
[11] I. Roytelman, B.K. Wee, R.L. Lugtu, Volt/var control algorithm for modern distribution management system, IEEE Trans. Power Syst. 10 (3) (1995) 1454–1460.
[12] D. Sochuliakova, D. Niebur, C.O. Nwankpa, R. Fischl, D. Richardson, Identification of capacitor position in a radial system, IEEE Trans. Power Del. 14 (4) (1999) 1368–1373.
[13] S. Santoso, J.D. Lamoree, M.F. McGranaghan, Signature analysis to track capacitor switching performance, in: Proceedings of 2001 IEEE Transmission and Distribution Conference, Atlanta, GA, 2001, pp. 259–263.